AIAA 2000–0358

Diode-Laser Absorption Sensor for Measurements in Pulse Detonation Engines

Scott T. Sanders, Thomas P. Jenkins, Jeffrey A. Baldwin,
Douglas S. Baer and Ronald K. Hanson
High Temperature Gasdynamics Laboratory
Mechanical Engineering Department
Stanford University, Stanford, CA 94305-3032 USA

38th AIAA Aerospace Sciences Meeting and Exhibit
January 10–13, 2000/Reno, NV

DIODE-LASER ABSORPTION SENSOR FOR MEASUREMENTS IN PULSE DETONATION ENGINES

S.T. Sanders*, T.P. Jenkins**, J.A. Baldwin*, D.S. Baer†, and R.K. Hanson‡
High Temperature Gasdynamics Laboratory
Department of Mechanical Engineering
Stanford University, Stanford, CA 94305-3032 USA

A diode laser sensor based on absorption spectroscopy techniques has been developed for *in situ* measurements of gas temperature, H_2O concentration, and soot volume fraction in pulse detonation engine (PDE) flows. The sensor employs 5 DFB diode lasers operating in the 1300-1800 nm spectral region. Gas temperature is determined from the ratio of H_2O absorbances at different wavelengths; water mole fraction and soot volume fraction are determined from the measured gas temperature and absorbances at selected wavelengths. The sensor's time response (0.5 μs) and non-intrusive nature make it suitable for measurements in the hostile environment generated by PDEs. The sensor has been demonstrated in a 3.8 cm diameter PDE detonating a JP-10 / O_2 aerosol. The engine performance information recorded by the sensor is expected to enhance PDE modeling and optimization, eventually enabling PDE combustion control.

Introduction

Pulse detonation engines have recently received increased attention in the aeropropulsion community, owing to their high theoretical specific impulse and structural simplicity [1]. Experimental studies of PDEs have been previously founded primarily on pressure data. Sensors for other engine properties of interest have been needed but generally unavailable.

The PDE is a challenging measurement environment because of its high pressures (up to 100 atm), high temperatures (up to 4000 K), and multiphase flowfield (soot and liquid fuel droplets are possible). Under these conditions, absorption features are severely broadened, prohibiting traditional wavelength-tuning absorption spectroscopy techniques. In addition, reliable spectroscopic data for these conditions are sparse, creating a need for basic spectroscopic studies. Moreover, at PDE conditions, soot emits strong infrared radiation, creating an additive noise that must be removed from laser transmission signals. Soot and liquid fuel impose a wavelength-dependent extinction of the probe beams that must be distinguished from molecular absorption. Flowfield density gradients induce beamsteering effects, and stress-induced birefringence at PDE optical ports modulates transmitted laser intensities [2]. The PDE's unsteady nature exacerbates these difficulties by demanding high-bandwidth detection. The sensor described here has addressed these challenges and demonstrated the capacity to obtain quantitative *in situ* measurements of gas temperature, H_2O concentration, and soot volume fraction in PDEs.

Theory

The theoretical basis for determining gas temperature and species concentration in combustion flows from measured molecular absorbance at multiple wavelengths has been described previously [3-5]. In brief, the Beer-Lambert relation [6] is used to determine gas temperature from the ratio of measured H_2O absorbances at multiple wavelengths. Using an independent measurement of pressure, the water mole fraction is then determined from the measured absorption at a selected wavelength using the known absorption line strength at the measured temperature.

Calculated near-IR absorption spectra for equilibrium products of stoichiometric JP-10 / O2 at representative PDE conditions of T = 3000 K and P = 15 atm are shown in Fig 1. Based on simulated spectra such as these, the H_2O-resonant wavelengths λ_1 = 1343.297 nm ($\nu_1+\nu_3$ band), λ_2 = 1391.673 nm ($2\nu_1$, $\nu_1+\nu_3$ bands), and λ_3 = 1799.180 nm ($2\nu_2+\nu_3 \leftarrow \nu_2$ hot band) indicated in Fig 1 were chosen for maximum sensitivity to temperature over the 900 – 3300 K range. The nonresonant wavelengths λ_{nr1} = 1290 nm and λ_{nr2} = 1650 nm were chosen to monitor extinction due to JP-10 droplets and soot.

* Research Assistant, Student Member AIAA
** Research Associate
† Senior Research Scientist, Member AIAA
‡ Professor, Fellow AIAA

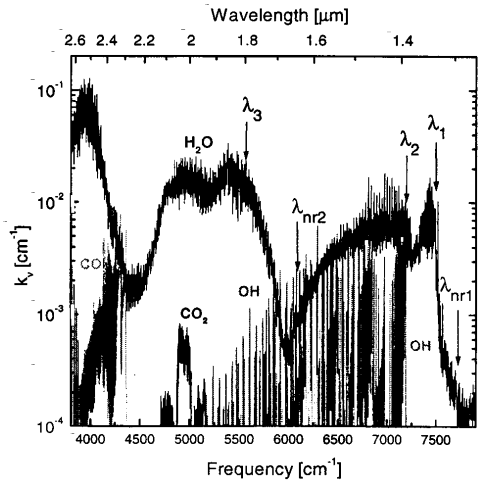

Figure 1. Calculated absorption spectra for equilibrium products of stojchiometric JP-10/O_2 at 3000K, 15 atm.

The volume fraction of Rayleigh-regime soot is determined from the extinction at a selected wavelength and an assumed refractive index [7] using established theory [8].

Spectroscopic Parameters

The spectroscopic parameters for the transitions near λ_1 and λ_2 have been detailed [9] and verified [5] previously. To maintain temperature sensitivity above 2000 K, a H_2O absorption feature near λ_3 was employed. A diode laser absorption measurement of this feature recorded in the product gases of an ethylene-air flame at T = 2050 K is shown in Fig 2. The measured feature was found to differ significantly from the HITRAN96/HITEMP [10] simulated feature shown gray in Fig 2. A 3-line model was therefore developed for this feature as an improvement over the HITEMP model. Line positions (ν_0) for the 3-line model were determined from diode laser absorption measurements of low-pressure H_2O in a heated static cell. Room temperature line strengths (S_{296}), lower state energies (E"), and broadening coefficients for a mixture of approximately 10% H_2O, 12% CO_2, and 78% N_2 ($2\gamma_{comb,296}$) were determined from both static cell measurements and flame measurements and are listed in Table 1. The temperature exponent n used to relate room temperature broadening coefficients to those at elevated temperatures according to

$$2\gamma_{comb}(T) = 2\gamma_{comb,296}(296/T)^n \quad [1]$$

was assumed equal to 0.63 based on previous calculations [11]. The 3 Voigt lineshapes predicted by the model for the relevant conditions are shown dotted in Fig 2. The 3-line model data is compared to HITEMP data in Table 1.

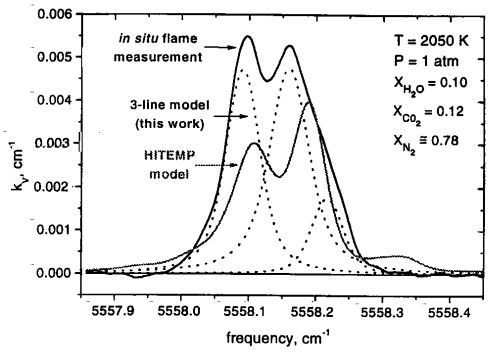

Figure 2. Absorption feature near λ_3.

	ν_0 [cm^{-1}]	S_{296} [cm^{-1}/atm]	E" [cm^{-1}]	$2\gamma_{comb,296}$
This work	5558.091	3.48×10^{-11}	5755	0.104
	5558.160	1.02×10^{-8}	4439	0.151
	5558.217	4.41×10^{-10}	4875	0.076
HITEMP	5558.106	1.29×10^{-3}	3225	0.093
	5558.129	1.28×10^{-6}	5749	0.093
	5558.188	1.93×10^{-5}	5242	0.038
	5558.188	1.11×10^{-4}	3940	0.056
	5558.203	6.44×10^{-6}	5242	0.038

Table 1. Spectroscopic data for feature near λ_3.

The 3-line model is not intended to provide fundamental spectroscopic parameters for the feature near λ_3. Rather, it was developed as a practical tool for measuring gas temperature in the high-temperature and high-pressure environment generated in PDEs.

The 3-line model is used to predict the spectral absorption coefficient k_v versus temperature at the frequency of 5558.090 cm^{-1}, as shown in Fig 3. The

model provides the desired spectral absorption coefficient to within ±2 percent for T < 2100 K. Agreement between the PDE gas temperature calculated using this model and the PDE soot temperature obtained by 2-color pyrometry suggests that the model provides k_ν at 5558.090 cm^{-1} to within ±10 percent to T ~ 3300 K.

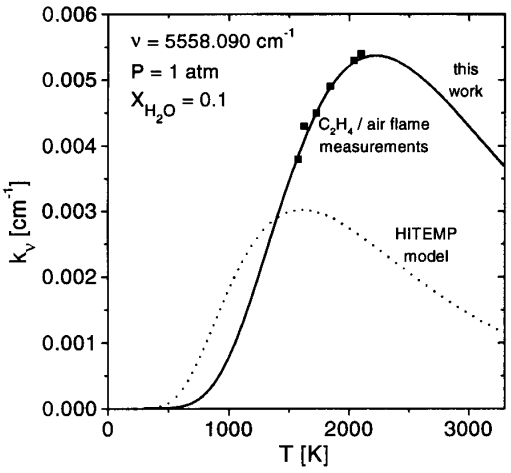

Figure 3. Variation of spectral absorption coefficient at 5558.090 cm^{-1} with temperature.

Experimental Method

The sensor was demonstrated in the 3.8 cm diameter pulsed detonation-initiation tube at the Naval Postgraduate School (NPS) in Monterey, CA, shown schematically in Fig 4 with a timing diagram. This PDE and the detonation pressure histories developed in it have been previously characterized [12]. Each cycle begins with an oxygen purge injected through the head end atomizer that lasts approximately 20 ms. Subsequently, a liquid JP-10 / oxygen aerosol is injected by the atomizer for ~20 ms. After a further delay of ~20 ms, the mixture is ignited by a capacitive discharge igniter 7 cm from the head end wall. The detonation wave builds and travels toward the tail end at approximately 2 km/s.

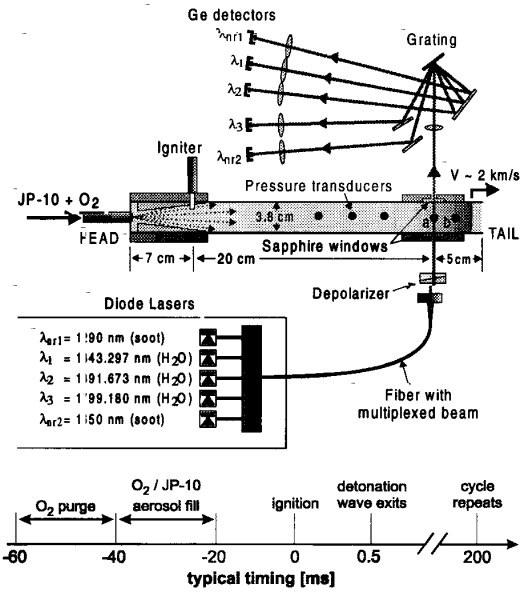

Figure 4. Experimental schematic and engine timing diagram.

Each of five DFB diode lasers in a remote control room send light via standard communications grade optical fiber (50 μm core) to the measurement station 5 cm from the tail end of the PDE. All lasers except the laser at λ_2 are operated at fixed wavelength; λ_2 is tuned at 30 kHz over the target H_2O absorption feature. The light passes through a depolarizer to mitigate the effects of stress-induced birefringence at the sapphire ports. The beam traverses the 3.8 cm path through the engine and is demultiplexed (into its component wavelengths) by a diffraction grating (830 g/mm, λ_b = 1.2 μm). The transmitted light is monitored by Germanium detectors (2 MHz bandwidth, 3mm dia.). The detector voltages were digitized using a 12-bit analog to digital (A/D) card installed in a personal computer.

In addition to demultiplexing the wavelengths, the grating rejects flowfield emission. However, during the high-pressure portions of the detonation cycle, blackbody radiation from soot was still able to contaminate the laser transmission signals. Whenever this occurred, the emission was further rejected by modulating the laser intensities at ~ 1 MHz with acousto-optic modulators and applying digital lock-in amplification to the recorded signals.

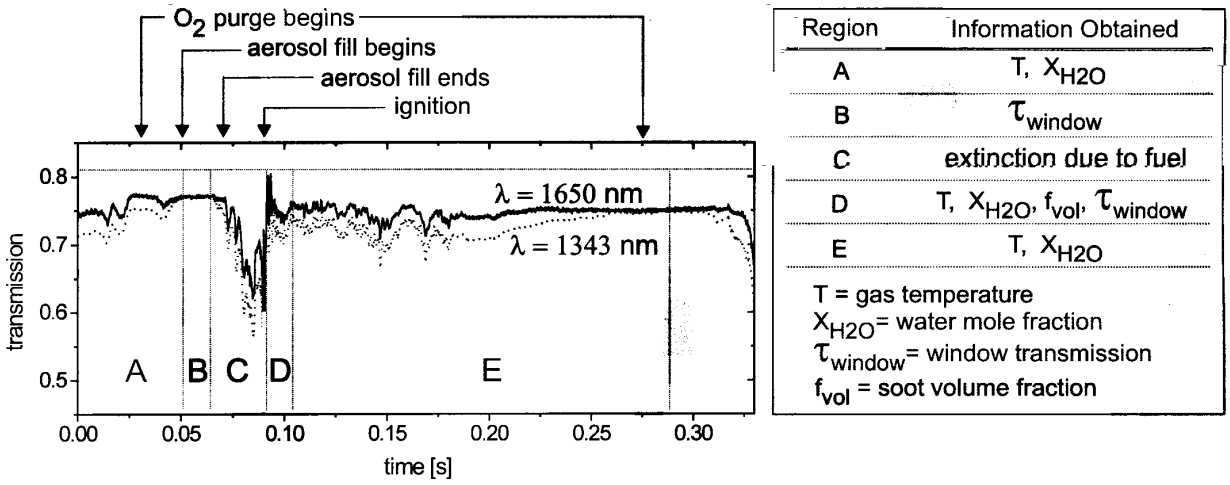

Figure 5. Raw transmission data at selected wavelengths and the information provided by the sensor during each pulse.

The grating and lenses in the transmitted-beam collection path have been arranged for minimum sensitivity to flow-induced beamsteering. By simulating beam steering using wedge windows, this collection system was found to be insensitive (to within 0.1%) to angular beam deflections of up to 2.6 degrees. The duration of non-negligible beamsteering associated with the passage of a detonation wave was found to be < 4 μs when this collection system was applied to the PDE at NPS.

Interpretation of optical results

A raw transmission versus time trace recorded during the eighth of fifteen consecutive engine pulses at 5 Hz is shown for two wavelengths in Fig 5, along with a list of the information the sensor provides. The 1343 nm wavelength is resonant, absorbed by H_2O and extinguished by soot and liquid fuel droplets. The 1650 nm wavelength is nonresonant, extinguished by soot and liquid fuel droplets but not absorbed by H_2O. A transmission of unity corresponds to a case where the optical access windows are perfectly clean (free of soot deposits) and no soot particles, fuel droplets, or H_2O are in the beam path (i.e. the condition just prior to the aerosol fill of the first pulse in the series).

During region "A" of Fig 5, soot and combustion gases from the previous pulse remain in the beam path and the windows are sooted, accounting for a nonunity transmission. The indicated oxygen purge is initiated at the head end and begins to displace the soot and combustion gases.

In region "B", the oxygen purge has displaced the soot and combustion gases from the flow, leaving a transmission of ~77% due solely to the sooted windows. In region "C", the beam path becomes occupied by JP-10 droplets, JP-10 vapor, and oxygen as the charge reaches the test station. Scattering from JP-10 droplets is the primary cause for the laser extinction in this region.

Region "D" begins with the passage of the detonation wave through the aerosol. The droplets are expected to shatter, vaporize, and combust within the first microsecond following wave passage [13]. JP-10 droplets are therefore assumed absent in region "D" and until the next fuel fill, leaving flowfield H_2O, flowfield soot (assumed to be in the Rayleigh scattering regime [14]), and window soot deposits (assumed to be in the geometric scattering regime [15]) as the possible absorbers. As has been demonstrated in sooted-foil studies of detonation structures [16], the detonation wave has the ability to clean the access windows, so the window transmission established in region "B" is no longer applicable. The flowfield soot volume fraction and the window transmission are calculated versus time using the absorption at the two nonresonant wavelengths and a previous measurement of the refractive index of soot [7]. The absorbance due to H_2O for each of the resonant wavelengths is calculated as (recorded absorbance at resonant wavelength) - (theoretical absorbance at resonant wavelength due to measured soot volume fraction and window transmission). Calculated gas temperature and H_2O concentration follow directly from the H_2O absorbances.

Region "E" begins when the test section pressure is between 0.9 and 1.1 atm and the flow properties begin to change slowly enough that they can be faithfully monitored by the 30 kHz scans of λ_2. A scan-wavelength spectroscopy technique is used to obtain the absorbance at λ_2 in this region. Because

the H_2O feature is spectrally narrow (~0.3 cm^{-1}), this technique is immune to interference from flowfield or window soot. This advantage is critical, since the assumption of Rayleigh-regime soot becomes inappropriate in region "E", prohibiting the soot interference subtraction scheme used in region "D". The absorbance at λ_1 can be obtained, however, using a modified soot subtraction scheme: the transmission near λ_2 but at the far wing of the H_2O feature and the transmission at λ_{nr1} are interpolated to obtain the appropriate absorbance due to soot at λ_1. The absorbance due to H_2O at λ_1 is then readily obtained, and gas temperature and H_2O concentration are determined as before.

Results and discussion

Typical pressure, gas temperature, and H_2O concentration results are shown versus time for the first three of fifteen consecutive engine pulses at 5 Hz in Fig 6. The indicated wave speeds were determined from the pressure pulse arrival times at transducers "a" and "b" labeled in Fig 4. Calculated Chapman-Jouget detonation properties for stoichiometric JP-10 / oxygen detonation are shown in Table 2. As was typical for this engine, the test-section wave speed is much lower for the first pulse than for subsequent pulses.

High-pressure gases exist at the test plane for approximately 500 μs following each detonation. High temperature H_2O typically remains at the test plane for a much longer time (>100 ms), due to combustion occurring in the blowdown following each detonation. Blowdown combustion interferes with a subsequent pulse's aerosol loading, limiting the maximum pulse rate for this PDE to approximately 10 Hz. Because this sensor clearly reveals combustion during a pulse's blowdown, it should prove useful in maximizing PDE cycle frequency (and thus maximizing thrust).

Vwave	2.3 km/s
T^a	3900 K
P^a	40 atm
$X_{H2O}{}^a$	0.20

[a]burned gas properties

Table 2. Chapman-Jouget properties for stoichiometric JP-10/oxygen detonation.

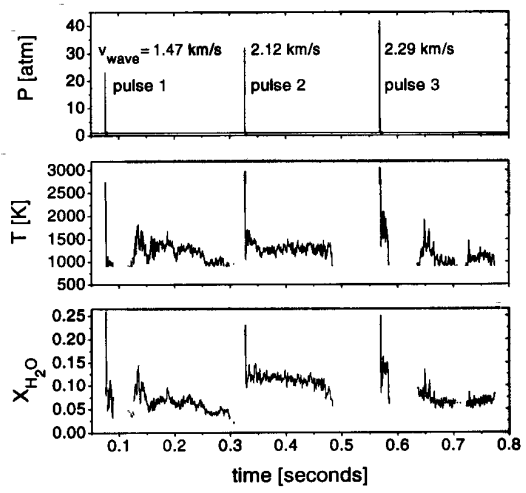

Figure 6. Properties recorded in the PDE at NPS for the first 3 of 15 consecutive engine pulses at 5 Hz.

When the temperature drops below 900 K or the water mole fraction below 0.01, results become inaccurate and are not presented. For all results presented in this work, the uncertainty is estimated at ±10%, typically limited by the variation in optical fiber transmission as it vibrates in the acoustic output of the PDE.

Properties measured during pulse 1 of Fig 6 are presented in Fig 7 with high time resolution. Gas temperature remains near 2500 K (64% of T_{CJ}) as the pressure decreases to near atmospheric. The temperature plummets rapidly to near 1000 K approximately 650 μs after the detonation wave passes the test plane. This is very near the calculated time of 600 μs required for the detonation wave to exit the tube and allow a rarefaction wave to propagate back to the test plane against the output flow; this rarefaction wave is likely responsible for the rapid gas cooling. *In situ* two-color emission pyrometry results recorded at the same test plane agree well with the sensor's record of gas temperature. Soot volume fraction (f_{vol}) and H_2O concentration results indicate the presence of combustion products within 4 μs of wave passage.

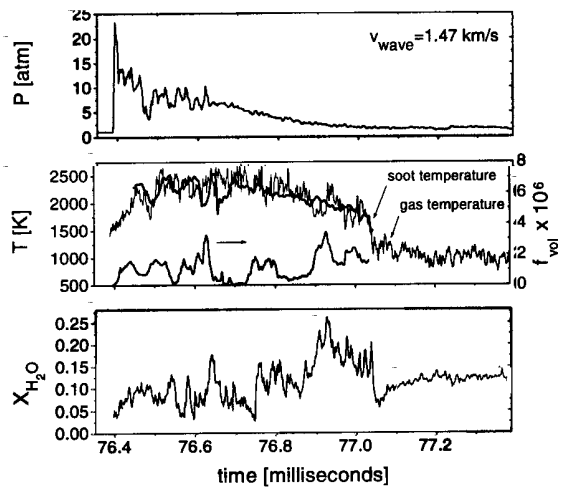

Figure 7. High resolution record of results from pulse 1 in Fig 6.

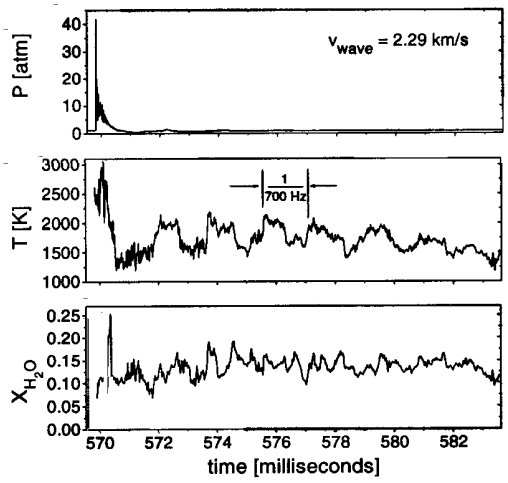

Figure 8. High resolution record of results for pulse 3.

Results from pulse 3 of Fig 6 are shown in Fig 8 with high time resolution. The peak pressure, wave speed, gas temperature, and H_2O concentration are significantly higher than in pulse 1. An increased JP-10 vapor concentration in the charge, due to higher charge temperature or leftover fuel vapor from the previous pulse, is believed responsible for this improved performance. This wave exhibits a speed and peak pressure within 5% of Table 2 predictions, even though the burned gas temperature and H_2O concentration remain significantly lower than CJ predictions. The 700-Hz temperature oscillations in the blowdown following this pulse are driven by flow direction oscillations at the test plane. Numerical studies of PDEs predict such oscillations [17]. The measured frequency is in agreement with a calculated frequency of 750 Hz based on a 1-D acoustic analysis.

Conclusions

A diode-laser based sensor has been developed for and applied to PDE flows. The sensor has demonstrated the capacity to obtain quantitative, *in situ* measurements of gas temperature, H_2O concentration, and soot volume fraction in a liquid-fuel-based detonation tube. The sensor reveals information that should prove useful in PDE modeling, optimization, and control strategies.

Acknowledgements

This work was sponsored by ONR, with Dr. Gabriel Roy as technical monitor, under the ONR MURI on PDEs. The authors gratefully acknowledge Professors C. M. Brophy and D. W. Netzer at the Naval Postgraduate School, Monterey, CA, for valuable discussions on PDE performance and for hosting our visit to demonstrate this sensor in the Rocket Propulsion and Combustion Laboratory.

References

1. Eidelman, S., *33rd AIAA Joint Propulsion Conference, AIAA paper #97-2740*, 1997.
2. Petersen, E.L., Bates, R.W., Davidson, D.F., and Hanson, R.K., *21st International Symposium on Shock Waves*, Vol. 1, 1997, pp. 459-464.
3. Philippe, L.C. and Hanson, R.K., *Applied Optics* 32:6090-6103 (1993).
4. Arroyo, M.P., Birbeck, T.P., Baer, D.S., and Hanson, R.K., *Optics Letters* 19:1091-1093 (1994).
5. Baer, D.S., Nagali, V., Furlong, E.R., Hanson, R.K., and Newfield, M.E., *AIAA Journal* 34:489-493 (1996).
6. Eckbreth, A.C., *Laser Diagnostics for Combustion Temperature and Species*, Gordon & Breach, Amsterdam, 1996.
7. Dalzell, W.H. and Sarofim, A.F., *Journal of Heat Transfer* 91:100-104 (1969).
8. Hottel, H.C. and Sarofim, A.F., *Radiative transfer*, McGraw-Hill, New York, 1967.
9. Toth, R.A., *Applied Optics* 33:4851-4867 (1994).

10. Rothman, L.S., et. al., *J. Quant. Spectrosc. Radiat. Transfer* 60:665-710 (1998).
11. Delaye, C., Hartmann, J., and Taine, J., *Applied Optics* 28:5080-5086 (1989).
12. Brophy, C.M. and Netzer, D.W., *35th AIAA Joint Propulsion Conference*, Los Angeles, CA, 1999.
13. Sanders, S.T., Unpublished Calculations, 1999.
14. Bohm, H., Feldermann, C., Heidermann, T., Jander, H., Luers, B., and Wagner, H.G., *Twenty-Fourth Symposium (International) on Combustion*, 1992, pp. 991-998.
15. Brugman, T.M., Stoffels, G.G.M., Dam, N., Meerts, W.L., and ter Meulen, J.J., *Applied Physics B* 64:717-724 (1997).
16. Auffret, Y., Desbordes, D., and Presles, H.N., *Shock Waves* 9:107-111 (1999).
17. Kailasanath, K., Patnaik, G., and Li, C., *AIAA Joint Propulsion Conference, AIAA paper #99-2634*, Los Angeles, CA, 1999.